

# REPORT DOCUMENTATION PAGE

Form Approved  
OMB No. 0704-0188

Public reporting burden for this collection of information is estimated to average 1 hour per response, including the time for reviewing instructions, searching existing data sources, gathering and maintaining the data needed, and completing and reviewing this collection of information. Send comments regarding this burden estimate or any other aspect of this collection of information, including suggestions for reducing this burden to Department of Defense, Washington Headquarters Services, Directorate for Information Operations and Reports (0704-0188), 1215 Jefferson Davis Highway, Suite 1204, Arlington, VA 22202-4302. Respondents should be aware that notwithstanding any other provision of law, no person shall be subject to any penalty for failing to comply with a collection of information if it does not display a currently valid OMB control number. PLEASE DO NOT RETURN YOUR FORM TO THE ABOVE ADDRESS.

1. REPORT DATE (DD-MM-YYYY) 06-01-2010		2. REPORT TYPE REPRINT		3. DATES COVERED (From - To)	
4. TITLE AND SUBTITLE Experimental and theoretical study of the reaction of $\text{POCl}_3^-$ with $\text{O}_2$				5a. CONTRACT NUMBER	
				5b. GRANT NUMBER	
				5c. PROGRAM ELEMENT NUMBER 62601F	
6. AUTHOR(S) S.K. Kerkines*, K. Morokuma*, N. Ioradanova** and A. Viggiano				5d. PROJECT NUMBER 1010	
				5e. TASK NUMBER BM	
				5f. WORK UNIT NUMBER A1	
7. PERFORMING ORGANIZATION NAME(S) AND ADDRESS(ES) Air Force Research Laboratory 29 Randolph Road Hanscom AFB MA 01731-3010				8. PERFORMING ORGANIZATION REPORT NUMBER  AFRL-RV-HA-TR-2010-1007	
9. SPONSORING / MONITORING AGENCY NAME(S) AND ADDRESS(ES)				10. SPONSOR/MONITOR'S ACRONYM(S)  AFRL/VSBXT	
				11. SPONSOR/MONITOR'S REPORT NUMBER(S)	
12. DISTRIBUTION / AVAILABILITY STATEMENT Approved for Public Release; Distribution Unlimited					
13. SUPPLEMENTARY NOTES REPRINTED FROM: J. Chemical Physics, 132, 044309 (2010) Copyright: 2010 American Inst Physics *Dept Chemistry, Emory Univ, Atlanta, GA, **Georgia Southwestern Univ, Americus, GA					
14. ABSTRACT  The oxidation of the trichlorooxyphosphorus anion ( $\text{POCl}_3^-$ ), which takes place in combustion flames, has been examined experimentally at a variety of temperatures and theoretically via <i>ab initio</i> and density functional methods. The reaction was examined in a turbulent ion flow tube and kinetics was measured between 300 and 626 K, estimating an overall reaction barrier of 1.23 kcal/mol. Calculations at the density functional, Møller-Plesset second order perturbation, and coupled cluster levels of theory with basis sets up to augmented triple- $\zeta$ quality point to a multistep reaction mechanism involving an initial $[\text{OP}(\text{Cl})_3(\text{OO})]^-$ intermediate, an adduct between triplet $\text{O}_2$ with $\text{POCl}_3^-$ , subsequent formation of a four-membered nonplanar $\text{P}-\text{O}-\text{O}-\text{Cl}$ ring transition state, with concomitant breaking of the $\text{P}-\text{Cl}$ and $\text{O}-\text{O}$ bonds to provide a transient intermediate $[\text{OP}(\text{Cl})_2\text{OO}\cdots\text{Cl}]^-$ , which, in turn, converts to the product complex $(\text{POCl}_2^-)(\text{ClO})$ upon formation of the $\text{Cl}-\text{O}$ bond without barrier. The calculated energy of the four-membered transition state is considered to be in good agreement with the small overall barrier found by experiment. The final step is responsible for the large exothermicity of the reaction. © 2010 American Institute of Physics.					
15. SUBJECT TERMS Ab initio calculations      Bonds (chemical)      Combustion, Density functional theory Flames      Ion-molecule reactions      Negative ions      Oxygen compounds      Perturbation theory					
16. SECURITY CLASSIFICATION OF:		17. LIMITATION OF ABSTRACT		18. NUMBER OF PAGES	
a. REPORT UNCLAS		b. ABSTRACT UNCLAS		19a. NAME OF RESPONSIBLE PERSON A.A. Viggiano	
				19b. TELEPHONE NUMBER (include area code)	

20100315116

Experimental and theoretical study of the reaction of  $\text{POCl}_3^-$  with  $\text{O}_2$ Ioannis S. K. Kerkines,<sup>1,a)</sup> Keiji Morokuma,<sup>1,b)</sup> Nedialka Iordanova,<sup>2</sup> and A. A. Viggiano<sup>3,c)</sup><sup>1</sup>Department of Chemistry and Cherry L. Emerson Center for Scientific Computation, Emory University, Atlanta, Georgia 30322, USA<sup>2</sup>Department of Chemistry, Georgia Southwestern State University, Americus, Georgia 31709, USA<sup>3</sup>Space Vehicles Directorate, Air Force Research Laboratory, Hanscom Air Force Base, Massachusetts 01731, USA

(Received 20 October 2009; accepted 6 January 2010; published online 27 January 2010)

The oxidation of the trichlorooxyphosphorus anion ( $\text{POCl}_3^-$ ), which takes place in combustion flames, has been examined experimentally at a variety of temperatures and theoretically via *ab initio* and density functional methods. The reaction was examined in a turbulent ion flow tube and kinetics was measured between 300 and 626 K, estimating an overall reaction barrier of 1.23 kcal/mol. Calculations at the density functional, Møller–Plesset second order perturbation, and coupled cluster levels of theory with basis sets up to augmented triple- $\zeta$  quality point to a multistep reaction mechanism involving an initial  $[\text{OP}(\text{Cl})_3(\text{OO})]^-$  intermediate, an adduct between triplet  $\text{O}_2$  with  $\text{POCl}_3^-$ , subsequent formation of a four-membered nonplanar  $\text{P}-\text{O}-\text{O}-\text{Cl}$  ring transition state, with concomitant breaking of the  $\text{P}-\text{Cl}$  and  $\text{O}-\text{O}$  bonds to provide a transient intermediate  $[\text{OP}(\text{Cl})_2\text{OO}\cdots\text{Cl}]^-$ , which, in turn, converts to the product complex  $(\text{POCl}_2^-(\text{ClO}))$  upon formation of the  $\text{Cl}-\text{O}$  bond without barrier. The calculated energy of the four-membered transition state is considered to be in good agreement with the small overall barrier found by experiment. The final step is responsible for the large exothermicity of the reaction. © 2010 American Institute of Physics. [doi:10.1063/1.3299276]

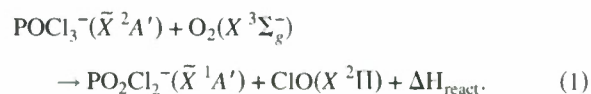
## I. INTRODUCTION

Goodings and his colleagues<sup>1,2</sup> showed that addition of  $\text{POCl}_3$  to flames results in  $\text{PO}_2^-$  and  $\text{PO}_3^-$  terminal ions. In order to help explain those results, we have studied a variety of the ion-molecule steps involved in the oxidation. Electron attachment produces  $\text{POCl}_3^-$  and  $\text{POCl}_2^-$ .<sup>3–5</sup> The chemistry of these ions was studied with a number of simple stable neutrals and found to be unreactive with species such as  $\text{O}_2$ ,  $\text{CO}_2$ , and  $\text{H}_2\text{O}$ .<sup>6</sup> Therefore, the oxidation from electron attachment products to  $\text{PO}_2^-$  and  $\text{PO}_3^-$  must involve minor species including unstable neutrals. Partial oxidation was found in reactions with ozone.<sup>7</sup>  $\text{POCl}_3^-$ ,  $\text{POCl}_2^-$ , and  $\text{PO}_2\text{Cl}^-$  were found to react with  $\text{O}_3$  at greater than 30% of the collision rate. Several of the products showed an oxidation channel and the reaction of  $\text{PO}_2\text{Cl}^-$  with  $\text{O}_2$  was found to produce  $\text{PO}_3^-$  and  $\text{PO}_4^-$ . While the products in the latter reaction are fully oxidized, the ion is produced only in limited abundance. A series of reactions involving H atoms showed that Cl abstraction to produce HCl was common.<sup>8</sup> That study also showed that the  $\text{POCl}^-$  formed in the  $\text{POCl}_2^-$  reaction with H, reacted with both  $\text{O}_2$  and  $\text{O}_3$  to form  $\text{PO}_x\text{Cl}_y^-$  ions. Reactions of O and N atoms with  $\text{PO}_x\text{Cl}_y^-$  ions also produced ions with fewer Cl atoms.<sup>9</sup> Recently, a study in-

volving  $\text{PO}_x\text{Cl}_y^-$  with  $\text{O}_2(a^1\Delta_g)$  showed little chemistry.<sup>10</sup> While these studies showed pathways to full oxidation, the main route has not been found.

All the ion-molecule studies discussed above were performed in a selected ion flow tube (SIFT).<sup>11</sup> It is difficult to study reactions with rate constants smaller than  $\sim 10^{-12} \text{ cm}^3 \text{ s}^{-1}$  in a SIFT. Since  $\text{O}_2$  is a main species in atmospheric plasmas, such as in the flame experiments, this upper limit is not very restrictive. Slow reactions with  $\text{O}_2$  can change the chemistry due to its large abundance. For instance, it was postulated that if the  $\text{O}_2^+$  reaction with  $\text{N}_2$  proceeded with a rate constant of the order of  $10^{-17} \text{ cm}^3 \text{ s}^{-1}$ , various plasmas could be affected.<sup>12,13</sup> The turbulent ion flow tube (TIFT) in our laboratory is much more sensitive than the SIFT and it was shown that the reaction was much smaller than needed to affect atmospheric plasmas.<sup>13</sup>

For the reasons above, we have re-examined the reaction of  $\text{POCl}_3^-$  with  $\text{O}_2$  in the TIFT,



Reaction (1) is easily measurable in that apparatus and fast enough to affect atmospheric plasmas with  $\text{POCl}_3$  added, such as the experiments from the Goodings laboratory.<sup>1,2</sup> Here, we report kinetics between 300 and 626 K for reaction (1), the upper limit set by the stability of  $\text{POCl}_3^-$  at high temperature. The reaction of  $\text{POCl}_2^-$  with  $\text{O}_2$  was not measurable. Other  $\text{PO}_x\text{Cl}_y^-$  ions are hard to produce in the TIFT, so no attempt was made to study them.

<sup>a)</sup>Present address: Theoretical and Physical Chemistry Institute, The National Hellenic Research Foundation, 48 Vassileos Constantinou Ave., Athens 116 35, Greece.

<sup>b)</sup>Electronic mail: morokuma@emory.edu.

<sup>c)</sup>Electronic mail: albert.viggiano@hanscom.af.mil.

The detailed study of the reactivity of such oxyphosphorus compounds from a theoretical standpoint is a matter that has virtually been ignored in literature, notwithstanding the plethora of recent experimental data. Early work of such type has mostly been limited to the structures and energies of reactants and products<sup>7</sup> and other studies include interaction energies of  $\text{PO}_2\text{Cl}_2^-$  with  $\text{H}_2\text{O}$  and  $\text{HCl}$ ,<sup>14</sup> as well as hydrolysis reactions of the phosphate anion.<sup>15</sup> In our case, reaction (1) is unusual in that the strong  $\text{O}_2$  bond is broken.<sup>16,17</sup> Therefore, in order to gain insight into the reaction mechanism, detailed theoretical [*ab initio* and density functional theory (DFT)] calculations have also been performed to complement the experimental study.

## II. EXPERIMENTAL METHOD

The experiments were performed in a TIFT, which has been described in detail previously.<sup>18,19</sup> Therefore, only a brief description is given here, with emphasis on the experimental details relevant to the present study. Ions were created in a sidearm with a corona discharge. The source region was separated from the flow tube by a 1 mm orifice to prevent backstreaming into the source and unwanted chemistry involving N (from the discharge) and  $\text{N}_2$  from occurring. The source gas consisted of a small amount of  $\text{POCl}_3$  added to Ar. The source produced mainly a mixture of  $\text{POCl}_3^-$  and  $\text{POCl}_2^-$  by electron attachment.<sup>3-5</sup> Upon exiting the ion source, the ions were carried downstream through a 2.54 cm diameter flow tube by a large flow of  $\text{N}_2$  obtained from liquid  $\text{N}_2$  boil-off. The ions were sampled through a nose cone and skimmer into a quadrupole mass spectrometer. The entire instrument can be heated up to 700 K.  $\text{O}_2$  was added about 60 cm from the nose cone and thoroughly mixed in the turbulent flow by fan shaped devices near the  $\text{O}_2$  inlet. For these experiments, the instrument was operated at 100 Torr. This pressure was about 200 times higher than that used in the SIFT, resulting in longer reaction times and larger absolute number densities of neutral reagents. This, in turn, increased the sensitivity to small rate constants. In these experiments, the  $\text{O}_2$  concentration was about equal to the total buffer pressure in a typical SIFT experiment. Kinetics was measured at a fixed reaction time and the  $\text{O}_2$  concentration was varied.

The temperature of the flow tube was changed by a series of resistance heaters embedded in insulating blankets. Several zones were used for better temperature uniformity.  $\text{N}_2$  was preheated as explained previously. The upper temperature limit was determined by the fact that  $\text{POCl}_3^-$  diminishes with temperature and vanished much above 626 K.

Figure 1 shows three mass spectra. The top two panels show high resolution spectra taken at 100 °C with and without  $\text{O}_2$  added. At this temperature, the dominant ion in the absence of  $\text{O}_2$  was  $\text{POCl}_3^-$  and four isotopomers were present.  $\text{POCl}_2^-$  was also relatively abundant. These were the two main species formed by low energy electron attachment to  $\text{POCl}_3$ , which shows that the electron temperature was near thermal.<sup>3-5</sup> In addition, a small  $\text{PO}_2\text{Cl}_2^-$  signal was present in the spectrum without added  $\text{O}_2$  probably due to a 5 ppm  $\text{O}_2$  impurity in the  $\text{N}_2$  buffer or a small leak. A few

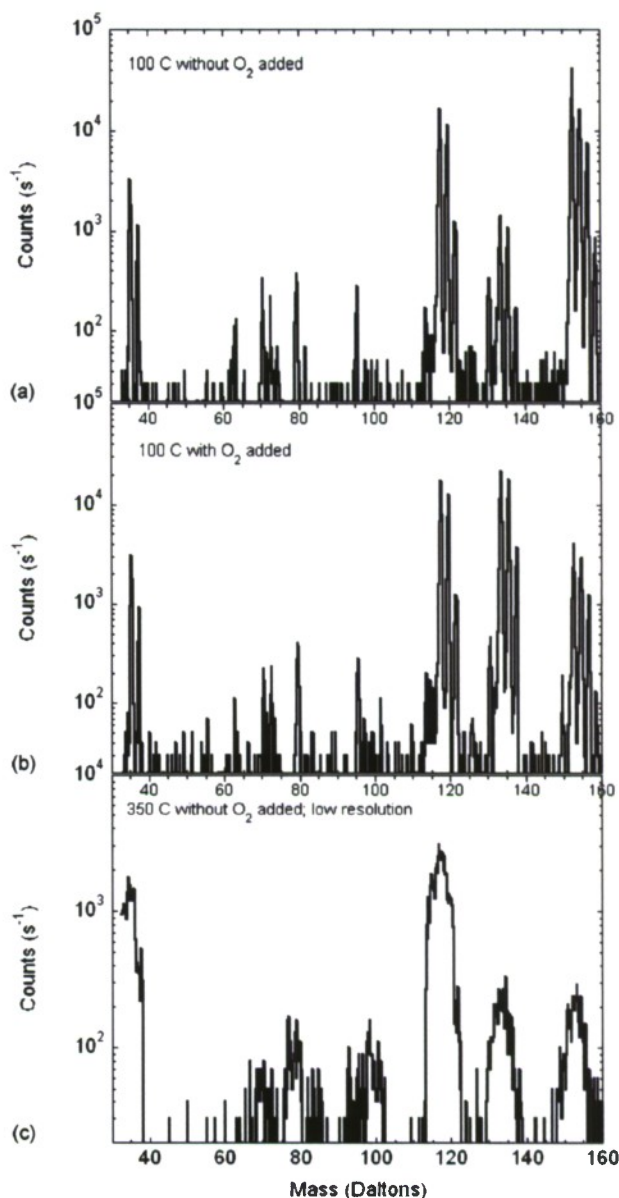
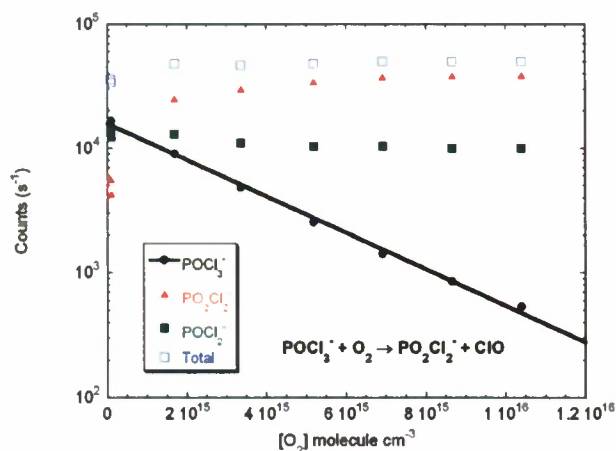


FIG. 1. High-resolution mass spectra taken at 100 °C (a) with, (b) without  $\text{O}_2$  added, and (c) at 350 °C with low mass resolution without  $\text{O}_2$  added.

percent of  $\text{Cl}^-$  was present. All other peaks were much smaller. The middle spectrum clearly shows that  $\text{O}_2$  addition converts  $\text{POCl}_3^-$  into  $\text{PO}_2\text{Cl}_2^-$ , leaving the other peaks essentially unchanged. The bottom spectrum was taken at 350 °C with low mass resolution without  $\text{O}_2$  added. At this temperature, the  $\text{POCl}_3^-$  signal was small but still observable. The  $\text{POCl}_3^-/\text{PO}_2\text{Cl}_2^-$  ratio was about 1, which shows that the rate constant for reaction (1) increased at higher temperatures. More  $\text{Cl}^-$  was also observed.

## III. THEORETICAL APPROACH

Several trial geometries of the  $(\text{POCl}_3, \text{O}_2)^-$  system were considered and calculated initially at the DFT level of theory, employing the hybrid Becke three-parameter Lee–Yang–Parr exchange correlation functional (B3LYP) and the 6-31

FIG. 2. Plot of ion intensities vs  $\text{O}_2$  concentration for data taken at 300 K.

+G(d) basis set with the GAUSSIAN 03 package.<sup>20</sup> Stationary points found on the ground doublet ( $D_0$ ) potential energy hypersurface (PES) were characterized by harmonic frequency calculations. Connectivity of the optimized transition state structures with the corresponding reactants and products was verified by following the reaction coordinate backward and forward, respectively, using the intrinsic reaction coordinate method.<sup>21</sup> Once a qualitative reaction pathway was established, we proceeded to obtain more accurate geometries of all the structures using the spin-unrestricted second order Møller–Plesset perturbation theory (MP2). For the one-electron basis, we employed the correlation-consistent basis sets of double and triple- $\zeta$  quality, aug-cc-pV(D+d)Z and aug-cc-pV(T+d)Z.<sup>22,23</sup> Diffuse functions (“aug”) are crucial for correctly describing the anionic character of the system, while the “+d” basis was deemed necessary because of the presence of the second-row elements P and Cl, for which it has been previously shown that the extra “d” function cures significant convergence issues<sup>23</sup> as well as the BSSE especially in the DZ and TZ bases.<sup>24</sup>

To further increase the quality of our findings, single point coupled cluster singles and doubles + a perturbative estimate of triples [CCSD(T)] calculations were carried out on the MP2/aug-cc-pV(T+d)Z geometries using the same basis set. All correlated calculations keep the 23 lowest-in-energy orbitals (corresponding to the inner, nonvalence shells of P, Cl, and O) as “frozen” (core).

As mentioned already, we have used the GAUSSIAN 03 software package along the theoretical study.<sup>20</sup> Some initial PES scans were performed with the help of the GRM code.<sup>25</sup>

## IV. RESULTS

### A. Experimental

Figure 2 shows a plot of ion intensities versus  $\text{O}_2$  concentration for the data taken at 300 K. In this data set,  $\text{POCl}_3^-$  and  $\text{POCl}_2^-$  start at about equal intensities and the former decreases by over an order of magnitude and the latter is essentially constant.  $\text{PO}_2\text{Cl}_2^-$  shows a sharp rise. The 300 K rate constant is  $1.25 \times 10^{-14} \text{ cm}^3 \text{ s}^{-1}$ . The difference

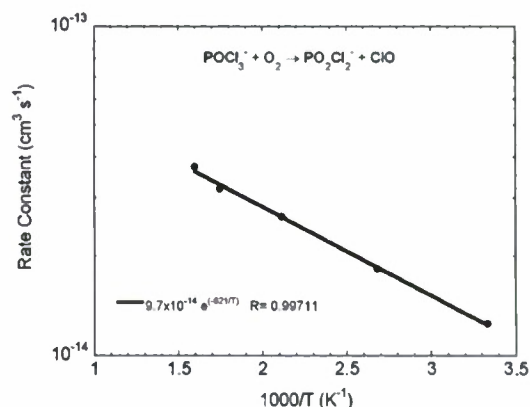


FIG. 3. Arrhenius plot of the results for five total temperatures over a 300–626 K temperature range.

in slopes between the two ions shows that small rate constants can easily be measured in the TIFT. No other ion intensity increased, and therefore the only product is  $\text{PO}_2\text{Cl}_2^-$ . Neutral products are not detected and are inferred from thermochemistry. To confirm the result, we measured rate constants with multiple isotopomers and found the same rate constant within a few percent. The error is estimated to be  $\pm 25\%$ .

The measurements were repeated for a total of five temperatures over the temperature range of 300–626 K. An Arrhenius plot of the results is shown in Fig. 3. The rate constant increases slowly with temperature, reaching a value of  $3.73 \times 10^{-14} \text{ cm}^3 \text{ s}^{-1}$  at 626 K. The estimated relative error is about 15% and the threefold increase over the entire temperature range is well outside the error. An activation energy of  $1.23 \text{ kcal mol}^{-1}$  is derived and the pre-exponential factor is approximately  $10^{-13} \text{ cm}^3 \text{ s}^{-1}$ . Reaction (1) is exothermic by about  $41 \text{ kcal mol}^{-1}$  (*vide infra*). Therefore, these results clearly show that there is a dynamical barrier to the reaction.

### B. Theoretical

A distinct feature of ion-molecule reactions of  $\{A+B\}^{+/-}$  type is that there are always two different reactant (and product) channels, either  $A^{+/-}+B$  or  $A+B^{+/-}$ ; therefore, the method chosen should at least be able to predict the correct ordering of ionization potentials or electron affinities of A and B.<sup>26</sup> It may get even more complicated when there are many energetically low-lying excited states or isomers of A and B which could interfere along the reaction pathway.

A number of possible reactants and products of this type have been considered for the  $\{\text{POCl}_3+\text{O}_2 \rightarrow \text{PO}_2\text{Cl}_2+\text{ClO}\}^-$  reaction on the ground doublet hypersurface and the relevant geometrical structures and energies at the B3LYP/6-31+G(d) level are shown in Table I and Fig. 4. Detailed discussion of the nature of each of these isomers is beyond the scope of this work. The experimental electron affinities of  $\text{POCl}_3$  and  $\text{O}_2$  are 1.4 and 0.451 eV, respectively,<sup>27,28</sup> so the lowest energy reactants are  $\text{POCl}_3^-(\bar{X}^2A')+\text{O}_2(X^3\Sigma_g^-)$ .

TABLE I. Total energies  $E(E_h)$ , ZPE (kcal/mol), ZPE-corrected relative energies  $\Delta E$  (kcal/mol), Mulliken atomic charges  $q$ , and spin densities ( $\rho$ ) of possible reactants and products for the  $[\text{POCl}_3 + \text{O}_2]^-$  reaction system at the B3LYP/6-31+G\* level of theory.

	E	ZPE	$\Delta E$	$q_P(\rho_P)$	$q_{O(1)}(\rho_{O(1)})$	$q_{O(2)}(\rho_{O(2)})$	$q_{Cl(1)}(\rho_{Cl(1)})$	$q_{Cl(2)}(\rho_{Cl(2)})$	$q_{Cl(3)}(\rho_{Cl(3)})$
$\text{POCl}_3\_S_0$	-1797.242 16	5.9	0.0	0.36	-0.42		0.02	0.02	0.02
$\text{POCl}_3\_T_0$	-1797.133 29	4.3	66.7	0.58(0.48)	-0.43(0.23)		-0.02(0.26)	-0.04(0.14)	-0.09(0.88)
$\text{POCl}_3^-\_D_0$	-1797.333 53	4.1	0.0	0.46(0.30)	-0.50(0.03)		-0.32(0.22)	-0.32(0.22)	-0.32(0.23)
$\text{POCl}_3^-\_D_1$	-1797.302 66	4.0	19.3	0.36(0.06)	-0.44(0.20)		-0.29(0.04)	-0.29(0.04)	-0.34(0.67)
$\text{POCl}_3^-\_D_2$	-1797.301 62	3.9	19.8	0.47(-0.01)	-0.46(0.29)		-0.33(0.03)	-0.33(0.03)	-0.34(0.67)
$\text{POCl}_3^-\_Q_0$	-1797.218 24	3.4	71.6	0.30(1.20)	-0.55(0.26)		-0.15(0.62)	-0.26(0.26)	-0.34(0.67)
$\text{PO}_2\text{Cl}_2\_D_0$	-1412.202 28	6.2	0.0	0.78(-0.09)	-0.38(0.52)	-0.38(0.52)	-0.01(0.02)	-0.01(0.02)	
$\text{PO}_2\text{Cl}_2\_D_1$	-1412.171 07	6.1	19.5	0.96(-0.01)	-0.49(0.00)	-0.49(0.00)	0.04(1.00)	-0.02(0.00)	
$\text{PO}_2\text{Cl}_2\_D_2$	-1412.144 99	5.7	35.5	0.82(0.53)	-0.37(-0.07)	-0.51(0.23)	0.13(0.16)	-0.07(0.15)	
$\text{PO}_2\text{Cl}_2\_D_3$	-1412.108 84	5.2	57.6	0.81(-0.01)	-0.51(0.10)	-0.40(0.01)	0.19(0.00)	-0.08(0.91)	
$\text{PO}_2\text{Cl}_2\_Q_0$	-1412.087 74	5.0	70.6	0.84(0.53)	-0.48(0.38)	-0.31(0.83)	0.02(1.05)	-0.07(0.21)	
$\text{PO}_2\text{Cl}_2^-\_S_0$	-1412.394 07	6.8	0.0	0.81	-0.62	-0.62	-0.28	-0.28	
$\text{PO}_2\text{Cl}_2^-\_T_0$	-1412.291 40	5.3	62.9	0.73(0.63)	-0.61(0.19)	-0.46(0.39)	-0.35(0.67)	-0.31(0.13)	
$\text{O}_2\_T_0$	-150.327 577	2.3	0.0		0.0(1.0)	0.0(1.0)			
$\text{O}_2\_S_0$	-150.266 052	2.3	38.6		0.0	0.0			
$\text{O}_2^-\_D_0$	-150.349 367	1.7	0.0		-0.5(0.5)	-0.5(0.5)			
$\text{ClO}_2\_D_0$	-535.300 093	1.2	0.0			-0.3(0.75)	0.3(0.25)		
$\text{ClO}_2\_Q_0$	-535.233 046	0.7	41.5			0.1(1.96)	-0.1(1.04)		
$\text{ClO}_2^-\_S_0$	-535.383 379	0.9	0.0			-0.8	-0.2		
$\text{ClO}_2^-\_T_0$	-535.368 596	0.4	8.8			-0.3(1.62)	-0.7(0.38)		

Even though B3LYP overestimates the electron affinity of  $\text{POCl}_3$  by about 1 eV (Table I), we consider this acceptable for our initial qualitative geometry scans, especially since the correct ordering of the electron affinities is predicted. B3LYP favors a symmetrical distorted-tetrahedron  $C_{3v}$   $\text{POCl}_3^-$  struc-

ture; however, at higher levels of theory, its symmetry is reduced to  $C_s$ , but the effect of reduced symmetry is not very large. The other structures of  $\text{POCl}_3^-$  correspond to  $[\text{POCl}_2 \cdots \text{Cl}]^-$  or  $[\text{POCl} \cdots \text{Cl} \cdots \text{Cl}]^-$  complexes and are about 20 kcal/mol or more higher in energy. The ground state

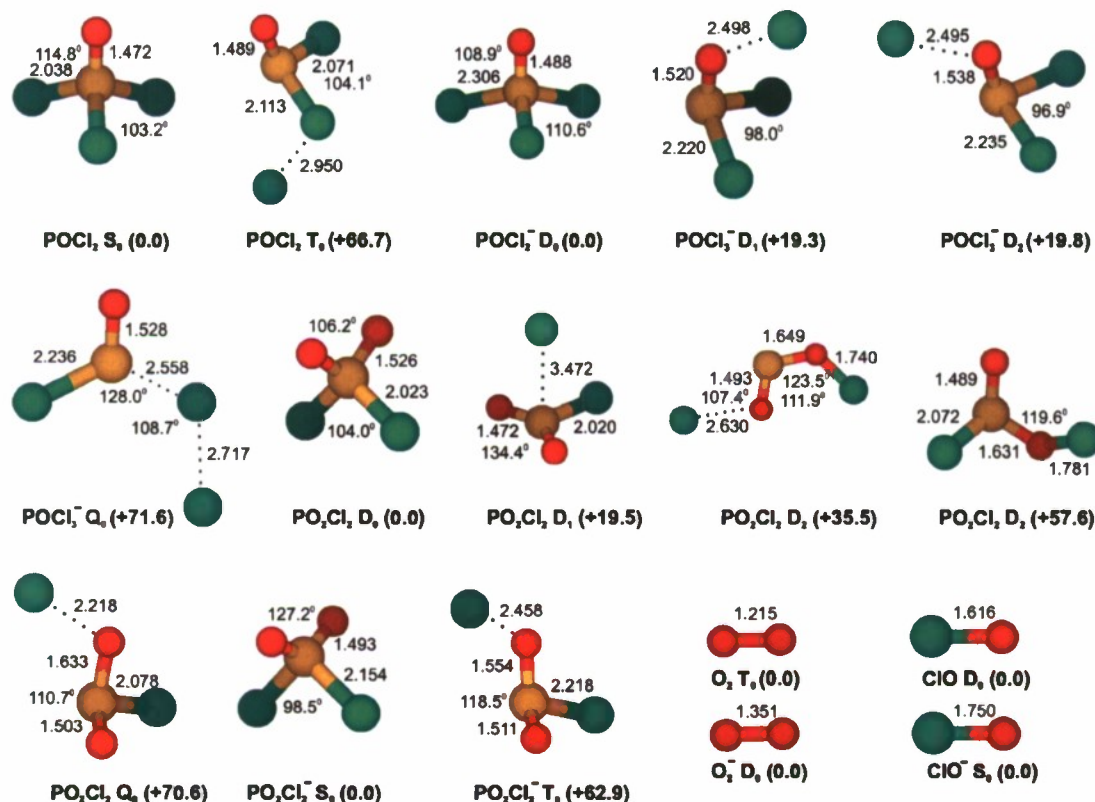


FIG. 4. The optimized structures (bond distances in angstroms and bond angles in degrees) and relative energies (with ZPE correction in kcal/mol) of possible reactants and products of the  $[\text{POCl}_3 + \text{O}_2]^-$  system at the B3LYP/6-31+G(d) level of theory.

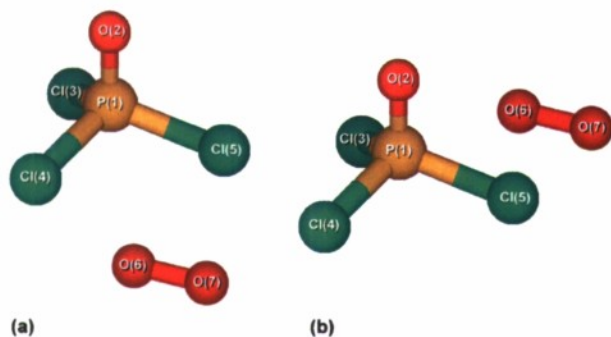
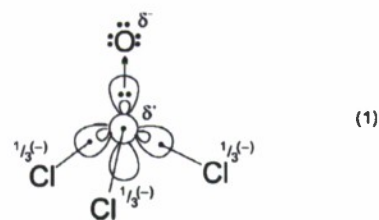


FIG. 5. Atomic numbering and schematic representation of the two possible approaches, (a) axial and (b) equatorial, of the  $\text{O}_2$  molecule to the  $\text{POCl}_3^-$  ion.

of neutral  $\text{POCl}_3$  ( $\text{POCl}_3\text{-}S_0$ ) is characterized by a polarized  $\text{P}\rightarrow\text{O}$  bond as Mulliken charge distributions indicate (Table I). No significant  $\text{O}\rightarrow\text{P}$   $p\pi\text{-}d\pi$  backbonding is observed. Comparing these charges with the ones in  $\text{POCl}_3^-$ , we see that the added negative charge is concentrated on the three Cl ligands of the phosphorus atom, leaving the polarity of the  $\text{P}\text{—}\text{O}$  bond practically intact, and especially the antibonding nature of the singly occupied molecular orbital (SOMO)

orbital results in the elongation of the three  $\text{P}\text{—}\text{Cl}$  bonds by about 0.3 Å in the anion versus the neutral (Fig. 4). The corresponding natural bond order charges show a similar

situation, but with even more polar  $\text{P}\text{—}\text{O}$  bonds ( $q_{\text{P}}=+1.59$ ,  $q_{\text{O}}=-0.98$  for  $\text{POCl}_3$ , and  $q_{\text{P}}=+1.41$ ,  $q_{\text{O}}=-1.04$  for  $\text{POCl}_3^-$ ). This is also confirmed by atomic spin density distributions (Table I), indicating that most of the excess spin is located on the three Cl atoms. A remaining 0.3 of spin remains on the P atom, which will facilitate the approach and bonding of triplet  $\text{O}_2$  in the first step of the reaction (*vide infra*). In both neutral and anion, the *in situ* P atom finds itself in its ground  $^4\text{S}$  state, offering its three lone pair electrons to the three Cl atoms and donating its (3s-like) lone electron pair to a  $^1\text{D}$  oxygen atom.<sup>29</sup> The following valence-bond-Lewis scheme attempts to condense these bonding characteristics in a qualitative way.



Chemical intuition also tells that a doublet  $\text{POCl}_3^-$  ion should react with triplet (but not with singlet)  $\text{O}_2$  by forming a pair of electrons resulting in an overall doublet state. Perpendicular approach of the  $X^3\Sigma_g^-$  oxygen molecule to the  $\text{POCl}_3^-$  positively charged P atom is expected to be attractive

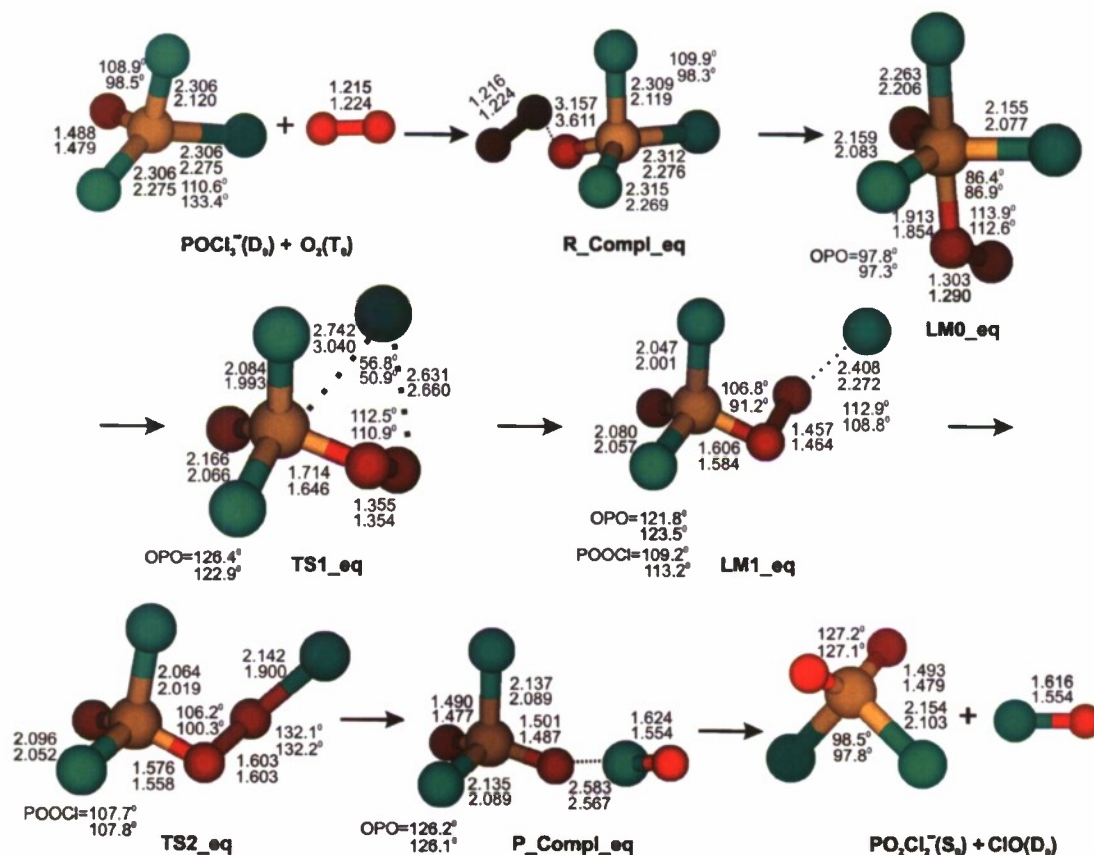


FIG. 6. Geometrical structures of reactants, intermediates, and products of the  $\text{POCl}_3^- + \text{O}_2$  reaction in the equatorial reaction pathway at the B3LYP/6-31+G(d) (upper numbers) and MP2/aug-cc-pV(T+d)/Z (lower numbers) levels of theory.

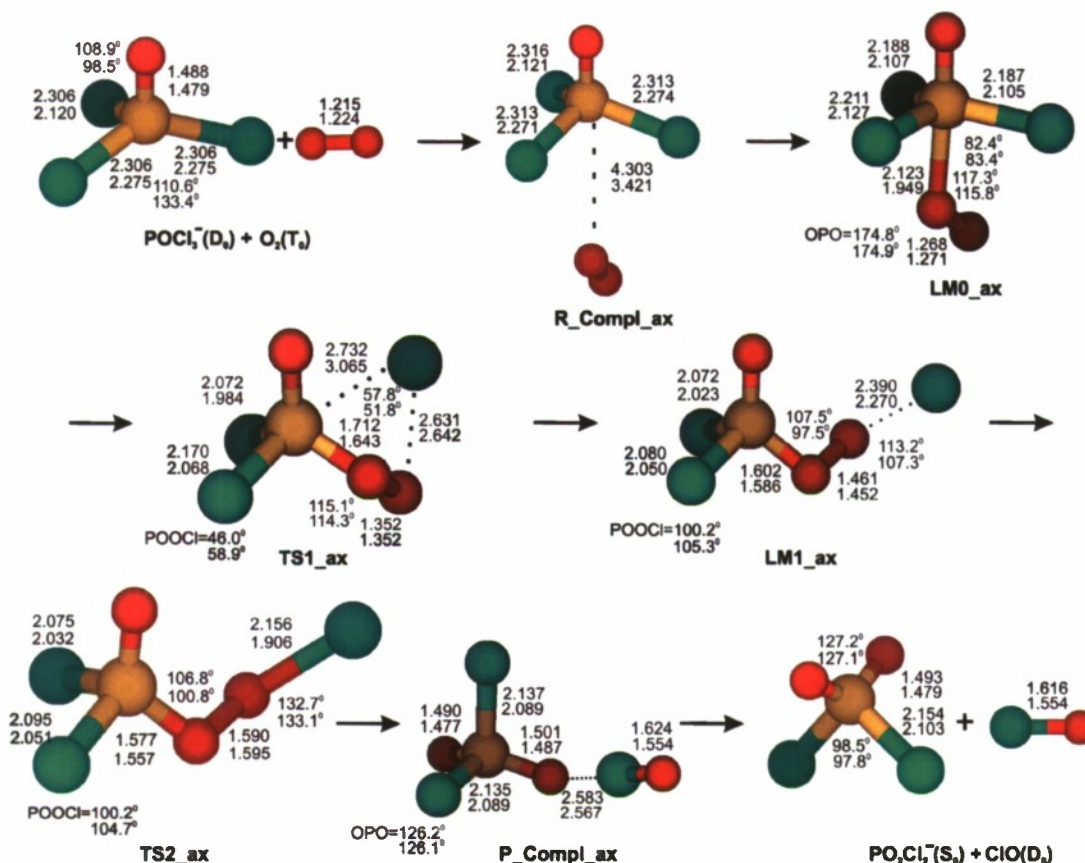
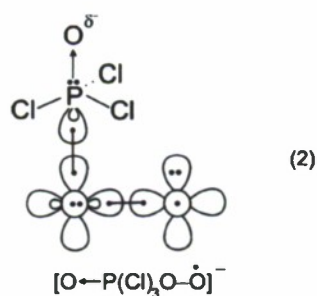


FIG. 7. Geometrical structures of reactants, intermediates, and products of the  $\text{POCl}_3^- + \text{O}_2$  reaction in the axial reaction pathway at the B3LYP/6-31+G(d) (upper numbers) and MP2/aug-cc-pV(T+d)/Z (lower numbers) levels of theory.

due an ion-dipole-induced Coulomb attraction, gradually leading to a  $\sigma$  electron coupling between a  $\pi^* \text{O}$  electron and the lone electron of  $\text{POCl}_3^-$  according to this scheme.



As shown in Fig. 5, two different orientations were considered for the attack of the triplet oxygen molecule to the doublet  $\text{POCl}_3^-$  ion in the overall doublet spin state, resulting in *axial* (ax) and *equatorial* (eq) and geometry configurations. In the former,  $\text{O}_2$  approaches parallel to the P—O axis of  $\text{POCl}_3^-$ , while in the latter, it does so in a parallel fashion to one of the P—Cl axes. For both orientations, similar pathways were determined (Figs. 6–8) involving the formation of at least two transition state complexes and two intermediates in addition to van der Waals reactant and product

complexes. The results for the equatorial and axial orientations at different levels of theory are tabulated in Tables II and III and are depicted in Figs. 6 and 7, respectively. Tables IV and V present Mulliken atomic charge and spin density distributions at the B3LYP/6-31+G\* level along both reac-

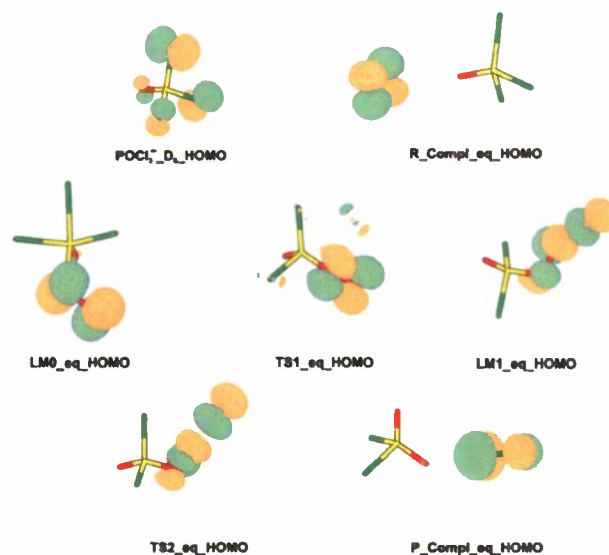


FIG. 8. Contour plots (threshold=0.05) of HOMO for selected chemical species of interest.

TABLE II. Stationary point relative energies (kcal/mol) at different levels of theory for the equatorial reaction pathway without and with zero-point energy differences ( $\Delta\text{ZPE}$ ).

	B3LYP/6-31+G*		UMP2/aug-cc-pV(T+d)Z		UCCSD(T)/aug-cc-pV(T+d)Z <sup>a</sup>	
	$\Delta E$	$\Delta E + \Delta\text{ZPE}$	$\Delta E$	$\Delta E + \Delta\text{ZPE}^b$	$\Delta E$	$\Delta E + \Delta\text{ZPE}^b$
Reactants	0.0 <sup>c</sup>	0.0	0.0 <sup>d</sup>	0.0	0.0 <sup>e</sup>	0.0
R_Compl_eq	-0.5	-0.4	-2.2	-1.2	-2.0	-1.0
TS0_eq	7.1	8.2	...	...	...	...
LM0_eq	3.3	5.5	-12.2	-9.2	-14.3	-11.2
TS1_eq	12.2	13.8	1.6	4.1	-3.5	-0.9
LM1_eq	0.5	2.7	-14.6	-6.9	-14.0	-6.3
TS2_eq	2.6	4.1	-5.9	-3.3	-11.6	-9.0
P_Compl_eq	-30.4	-28.3	-50.6	-48.1	-53.7	-51.2
Products	-20.7	-19.2	-39.4	-37.6	-43.1	-41.3

<sup>a</sup>At UMP2/aug-cc-pV(T+d)Z geometry.<sup>b</sup>With UMP2/aug-cc-pV(D+d)Z frequencies.<sup>c</sup> $E = -1947.661\,105\,E_h$ .<sup>d</sup> $E = -1945.457\,112\,E_h$ .<sup>e</sup> $E = -1945.575\,327\,E_h$ .

tion pathways. Depictions of the highest (singly) occupied molecular orbitals (HOMOs) for certain species of interest are presented in Fig. 8. Finally, Fig. 9 shows the schematic energetics for both reaction pathways.

## V. DISCUSSION

As expected and shown in scheme 2, a weak ion-molecule van der Waals reactant complex (R\_Compl) is converted to an side-on  $[\text{OP}(\text{Cl})_3(\text{OO})]^-$  intermediate (LM0) for both equatorial and axial orientations. This step bears many similarities to the known reaction mechanism between alkyl cations and  $\text{O}_3$ .<sup>30</sup> As mentioned already, LM0 is formed when  $\text{O}_2(X^3\Sigma_g^-)$  points one of its two  $\pi^*$  unpaired electrons toward the positively charged P atom and eventually forms a single  $\sigma$  bond as scheme 2 shows. The formation is barrierless at high levels of theory, although a transition state (TS0) was found at the B3LYP/6-31+G(d) level which could not be found at the MP2 level. According to Mulliken charge and atomic spin density distributions (Tables IV and V), an electron flux from the chlorine atoms toward dioxygen via phosphorus takes place. Indeed, the three chlorine atoms lose about  $\sim 0.35e^-$  upon formation of the P—O—O bond. The P atom also loses  $0.15e^-$ , enhancing the polarity of the pre-existing P—O bond. The reactants and the reactant complex (R\_Compl) have a total of three unpaired electrons coupled into a doublet ( $\alpha\alpha\beta$ ), which upon formation of LM0 are recoupled into a single-electron doublet, with the spin located on the O—O moiety, essentially on the other  $\pi^*$  orbital (Tables IV and V) and formally vertical to the P—O—O plane.

When zero-point energy differences ( $\Delta\text{ZPE}$ ) are taken into account, the formation of this P—O bond is exothermic by 11.2 kcal/mol for LM0\_eq, but only 0.9 kcal/mol for LM0\_ax at the CCSD(T)/aug-cc-pV(T+d)Z level of theory. There is also an  $\sim 0.01\text{ \AA}$  difference in the length of the formed P—O bond between these two isomers. Thus, an *axial effect* seems to be significant. Mulliken charges reveal that the O—O moiety attracts less electron charge in the more weakly bound LM0\_ax ( $0.26e^-$  versus  $0.4e^-$ ). The effect of the axial ligand is demonstrated by its Mulliken

TABLE III. Stationary point relative energies (kcal/mol) at different levels of theory for the axial reaction pathway without and with zero-point energy differences ( $\Delta\text{ZPE}$ ).

	B3LYP/6-31+G*		UMP2/aug-cc-pV(T+d)Z		UCCSD(T)/aug-cc-pV(T+d)Z <sup>a</sup>	
	$\Delta E$	$\Delta E + \Delta\text{ZPE}$	$\Delta E$	$\Delta E + \Delta\text{ZPE}^b$	$\Delta E$	$\Delta E + \Delta\text{ZPE}^b$
Reactants	0.0 <sup>c</sup>	0.0	0.0 <sup>d</sup>	0.0	0.0 <sup>e</sup>	0.0
R_Compl_ax	-0.3	-0.2	-2.2	-1.2	-1.9	-0.9
TS0_ax	9.4	10.9	...	...	...	...
LM0_ax	9.4	11.2	-2.3	0.8	-4.0	-0.9
TS1_ax	12.0	13.7	2.1	4.5	-3.4	-1.0
LM1_ax	1.6	3.8	-12.6	-6.2	-12.3	-5.9
TS2_ax	3.1	4.5	-4.7	-2.2	-10.5	-8.0
P_Compl_ax	-30.4	-28.3	-50.6	-48.1	-53.7	-51.3
Products	-20.7	-19.2	-39.4	-37.6	-43.1	-41.3

<sup>a</sup>At UMP2/aug-cc-pV(T+d)Z geometry.<sup>b</sup>With UMP2/aug-cc-pV(D+d)Z frequencies.<sup>c</sup> $E = -1947.661\,105\,E_h$ .<sup>d</sup> $E = -1945.457\,112\,E_h$ .<sup>e</sup> $E = -1945.575\,327\,E_h$ .

TABLE IV. Mulliken atomic charge and spin density distributions (in parentheses) at the B3LYP/6-31+G\* level of theory (*equatorial* reaction pathway).

	Atom	R_compl_eq	LM0_eq	TS1_eq	LM1_eq	TS2_eq	P_compl_eq
1	P	0.42(−0.29)	0.57(−0.01)	0.62(0.00)	0.79(0.00)	0.80(0.00)	0.78(0.00)
2	O	−0.48(−0.03)	−0.55(0.00)	−0.50(0.00)	−0.58(0.00)	−0.59(0.00)	−0.62(0.00)
3	Cl	−0.32(−0.22)	−0.16(−0.01)	−0.27(0.00)	−0.16(0.00)	−0.18(0.00)	−0.25(0.00)
4	Cl	−0.31(−0.22)	−0.16(−0.01)	−0.51(0.18)	−0.52(0.51)	−0.43(0.43)	0.34(0.28)
5	Cl	−0.32(−0.23)	−0.29(0.00)	−0.05(0.01)	−0.07(0.00)	−0.11(0.00)	−0.24(0.00)
6	O	0.03(1.03)	−0.15(0.35)	−0.22(0.13)	−0.22(0.04)	−0.30(0.07)	−0.62(0.00)
7	O	−0.02(0.97)	−0.25(0.67)	−0.07(0.67)	−0.24(0.45)	−0.18(0.49)	−0.39(0.71)

charge; in both axial and equatorial cases, the axial ligand (Cl or O) becomes more negatively charged due to the attack of O<sub>2</sub> to P.

The reaction from LM0 proceeds similarly for both axial and equatorial orientations. A four-membered nonplanar P⋯O—O⋯Cl ring transition state (TS1) is formed, essentially upon the transfer of one Cl atom from P to O, and the subsequent breaking of the P—Cl bond, to result in the formation of the second intermediate complex {OP(Cl)<sub>2</sub>OO⋯Cl}<sup>−</sup> (LM1) with a partially formed —O⋯Cl bond (Figs. 6 and 7). At the B3LYP/6-31+G(d) level, TS1 energetically lies significantly above the reactants (~14 kcal/mol) for both pathways. At the MP2/aug-cc-pV(D+d)Z level, both TS1<sub>eq</sub> and TS1<sub>ax</sub> have one imaginary frequency each (114i cm<sup>−1</sup> and 174i cm<sup>−1</sup>, respectively) with the much reduced energy of ~4–5 kcal/mol above the reactants. The energies of both TS1<sub>eq</sub> and TS1<sub>ax</sub> become slightly negative, from −1.0 to −0.9 kcal/mol relative to the reactants at our best CCSD(T)/aug-cc-pV(T+d)Z//MP2 level. These are the highest points on the doublet PES and correspond to the overall barriers of the reaction. There seems to be no preference between the equatorial and the axial pathways. This barrier can be compared with the experimentally observed barrier for the reaction of 1.23 kcal/mol. Although the sign is wrong, the very small calculated barrier is taken to be in satisfactory agreement with the experiment. The error of ~2.2 kcal/mol between the calculated and the experimental barriers may be attributed to the use of MP2 geometry, MP2 frequencies, and the basis set incompleteness in the CCSD(T) calculations.

The final step of the reaction takes place from LM1 via TS2, where the Cl atom with a long O⋯Cl bond is captured by the terminal oxygen atom and the elongated and weak-

ened O—O bond breaks forming an ion-molecule complex P\_Compl between the products: ClO(X<sup>2</sup>Π) and PO<sub>2</sub>Cl<sub>2</sub><sup>−</sup>. Mulliken atomic charges and spin densities for both equatorial and axial orientations confirm these observations (Tables IV and V). MP2/aug-cc-pV(D+d)Z gives a large imaginary frequency of 932i cm<sup>−1</sup> for TS2<sub>eq</sub> and 898i cm<sup>−1</sup> for TS2<sub>ax</sub>, indicating that TS2 is a real transition state at these levels, with the energy requirement of 3–4 kcal/mol from LM1 and is energetically below the reactants. However, at the CCSD(T)/aug-cc-pV(T+d)Z//MP2 level, when ΔZPE is taken into account, TS2 becomes lower in energy than LM1 and the transition state vanishes. The change in energy from LM1 to the product complex P\_Compl is very negative, dominating the large overall exothermicity of the reaction. The product complex P\_Compl dissociates into the isolated products POCl<sub>2</sub><sup>−</sup>+ClO with a energy requirement of ~10 kcal/mol and an overall exothermicity of 41.3 kcal/mol at the CCSD(T) level (Tables III and IV).

## VI. SUMMARY

The POCl<sub>3</sub><sup>−</sup>+O<sub>2</sub> reaction has been studied from both experimental and theoretical viewpoints. The main products of the reaction are PO<sub>2</sub>Cl<sub>2</sub><sup>−</sup>( $\tilde{X}^1A'$ )+ClO(X<sup>2</sup>Π). The reaction was examined in a TIFT, and kinetics was measured between 300 and 626 K. These measurements gave an overall reaction barrier of 1.23 kcal/mol.

Examination of the reaction pathways at different levels of theory points out to a multistep reaction mechanism, involving an initial [OP(Cl)<sub>3</sub>(OO)]<sup>−</sup> intermediate, an adduct between O<sub>2</sub> with POCl<sub>3</sub><sup>−</sup>, subsequent formation of a four-membered nonplanar P—O—O—Cl ring transition state, and with concomitant breaking of the P—Cl and O—O bonds to provide a transient intermediate

TABLE V. Mulliken atomic charge and spin density distributions (in parentheses) at the B3LYP/6-31+G\* level of theory (*axial* reaction pathway).

	Atom	R_compl_ax	LM0_ax	TS1_ax	LM1_ax	TS2_ax	P_compl_ax
1	P	0.44(−0.31)	0.68(−0.06)	0.62(0.00)	0.79(0.00)	0.79(0.00)	0.78(0.00)
2	O	−0.51(−0.03)	−0.68(0.00)	−0.49(0.01)	−0.54(0.00)	−0.56(0.00)	−0.62(0.00)
3	Cl	−0.32(−0.22)	−0.25(−0.04)	−0.28(0.00)	−0.16(0.00)	−0.18(0.01)	−0.25(0.00)
4	Cl	−0.31(−0.22)	−0.24(−0.03)	−0.50(0.19)	−0.51(0.53)	−0.43(0.45)	0.34(0.28)
5	Cl	−0.31(−0.22)	−0.24(−0.03)	−0.05(0.00)	−0.13(0.00)	−0.14(0.00)	−0.24(0.00)
6	O	0.04(1.03)	−0.06(0.49)	−0.17(0.14)	−0.21(0.03)	−0.29(0.07)	−0.63(0.00)
7	O	−0.03(0.97)	−0.20(0.68)	−0.13(0.66)	−0.24(0.44)	−0.19(0.47)	−0.39(0.71)

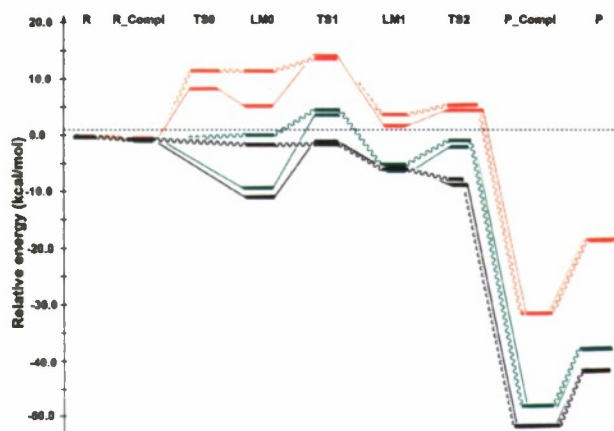


FIG. 9. Comparison of energetics (with ZPE correction) for the equatorial (straight lines) and axial (wiggly lines) pathways at different levels of theory (red: B3LYP/6-31G\*, green: MP2/aug-cc-pV(T+d)Z, black: CCSD(T)/aug-cc-pV(T+d)Z at MP2 geometry). The dashed line shows the experimental value of the energy barrier (1.23 kcal/mol).

$[\text{OP}(\text{Cl})_2\text{OO}\cdots\text{Cl}]^-$ , which converts to the product complex  $(\text{POCl}_2)^-(\text{ClO})$  upon formation of the Cl—O bond without barrier. The calculated energy of the four-membered transition state, the highest point on the potential profile at the highest level, is  $\sim -1.0$  kcal/mol, which is considered to be in good agreement with the small overall barrier by experiment. The final step is responsible for the large exothermicity of the reaction.

## ACKNOWLEDGMENTS

The present research was supported in part by grants from AFOSR (Grant No. FA9550-07-1-0395). N.I. acknowledges an Emerson Center Visiting Fellowship. Computer time was provided by a grant under the DoD-High Performance Computing Program and by Research Center for Computational Science, Okazaki, Japan, as well as by Cherry Emerson Center for Scientific Computation.

<sup>1</sup>J. M. Goodings and C. S. Hassanali, *Int. J. Mass Spectrom. Ion Process.* **101**, 337 (1990).

<sup>2</sup>J. H. Horton, P. N. Crovisier, and J. M. Goodings, *Int. J. Mass Spectrom. Ion Process.* **114**, 99 (1992).

<sup>3</sup>T. M. Miller, J. V. Seeley, W. B. Knighton, R. F. Meads, A. A. Viggiano, R. A. Morris, J. M. Van Doren, J. Gu, and H. F. Schaefer III, *J. Chem.*

*Phys.* **109**, 578 (1998).

<sup>4</sup>J. M. Van Doren, J. F. Friedman, T. M. Miller, A. A. Viggiano, S. Denifl, P. Scheier, T. D. Mark, and J. Troe, *J. Chem. Phys.* **124**, 124322 (2006).

<sup>5</sup>D. H. Williamson, C. A. Mayhew, W. B. Knighton, and E. P. Grimsrud, *J. Chem. Phys.* **113**, 11035 (2000).

<sup>6</sup>R. A. Morris and A. A. Viggiano, *Int. J. Mass Spectrom. Ion Process.* **164**, 35 (1997).

<sup>7</sup>A. I. Fernandez, A. J. Midey, T. M. Miller, and A. A. Viggiano, *J. Phys. Chem. A* **108**, 9120 (2004).

<sup>8</sup>A. J. Midey, T. M. Miller, R. A. Morris, and A. A. Viggiano, *J. Phys. Chem. A* **109**, 2559 (2005).

<sup>9</sup>J. C. Poutsma, A. J. Midey, T. H. Thompson, and A. A. Viggiano, *J. Phys. Chem. A* **110**, 11315 (2006).

<sup>10</sup>A. J. Midey, I. Dotan, and A. A. Viggiano, *Int. J. Mass Spectrom.* **273**, 7 (2008).

<sup>11</sup>A. A. Viggiano, R. A. Morris, F. Dale, J. F. Paulson, K. Giles, D. Smith, and T. Su, *J. Chem. Phys.* **93**, 1149 (1990).

<sup>12</sup>D. Sentman (personal communication).

<sup>13</sup>A. A. Viggiano, *J. Phys. Chem. A* **110**, 11599 (2006).

<sup>14</sup>H. Basch, M. Krauss, and W. J. Stevens, *J. Phys. Chem.* **95**, 7673 (1991).

<sup>15</sup>J. M. Mercer, P. Barrett, C. W. Lam, J. E. Fowler, J. M. Ugalde, and L. G. Pedersen, *J. Comput. Chem.* **21**, 43 (2000).

<sup>16</sup>V. Anichich, "An index of the literature for bimolecular gas phase cation-molecule reaction kinetics," Jet Propulsion Laboratory Report No. 03-19, 2003.

<sup>17</sup>Y. Ikezoe, S. Matsuoka, M. Takebe, and A. A. Viggiano, *Gas Phase Ion-Molecule Reaction Rate Constants Through 1986* (Maruzen Company, Tokyo, 1987).

<sup>18</sup>S. T. Arnold, J. V. Seeley, J. S. Williamson, P. L. Mundis, and A. A. Viggiano, *J. Phys. Chem. A* **104**, 5511 (2000).

<sup>19</sup>A. A. Viggiano, T. M. Miller, S. Williams, S. T. Arnold, J. V. Seeley, and J. F. Friedman, *J. Phys. Chem. A* **106**, 11917 (2002).

<sup>20</sup>M. J. Frisch, G. W. Trucks, H. B. Schlegel *et al.*, GAUSSIAN 03, Revision A1, 2003.

<sup>21</sup>K. Fukui, *Acc. Chem. Res.* **14**, 363 (1981).

<sup>22</sup>T. H. Dunning, Jr., *J. Chem. Phys.* **90**, 1007 (1989); D. E. Woon and T. H. Dunning, Jr., *ibid.* **98**, 1358 (1993).

<sup>23</sup>T. H. Dunning, Jr., K. A. Peterson, and A. K. Wilson, *J. Chem. Phys.* **114**, 9244 (2001).

<sup>24</sup>I. S. K. Kerkines and A. Mavridis, *J. Chem. Phys.* **123**, 124301 (2005).

<sup>25</sup>K. Ohno and S. Maeda, *Chem. Phys. Lett.* **384**, 277 (2004); S. Maeda and K. Ohno, *J. Phys. Chem. A* **109**, 5742 (2005); K. Ohno and S. Maeda, *ibid.* **110**, 8933 (2006); GRRM (Global Reaction Route Map), Version 1.00, 2007.

<sup>26</sup>A. J. Midey, A. A. Viggiano, P. Zhang, S. Irle, and K. Morokuma, *J. Phys. Chem. A* **110**, 3080 (2006); K. Fukuzawa, T. Matsushita, and K. Morokuma, *J. Chem. Phys.* **121**, 3117 (2004).

<sup>27</sup>B. P. Mathur, E. W. Rothe, S. Y. Tang, and G. P. Reck, *J. Chem. Phys.* **65**, 565 (1976).

<sup>28</sup>M. J. Travers, D. C. Cowles, and G. B. Ellison, *Chem. Phys. Lett.* **164**, 449 (1989).

<sup>29</sup>A. Kalemios and A. Mavridis, *J. Phys. Chem. A* **113**, 13972 (2009).

<sup>30</sup>S. Williams, W. B. Knighton, A. J. Midey, A. A. Viggiano, S. Irle, and K. Morokuma, *J. Phys. Chem. A* **108**, 1980 (2004).